ACS Chemical Neuroscience

Research Article

pubs.acs.org/chemneuro

Design and Synthesis of New Transient Receptor Potential Vanilloid Type-1 (TRPV1) Channel Modulators: Identification, Molecular Modeling Analysis, and Pharmacological Characterization of the *N*-(4-Hydroxy-3-methoxybenzyl)-4-(thiophen-2-yl)butanamide, a Small Molecule Endowed with Agonist TRPV1 Activity and Protective Effects against Oxidative Stress

Francesca Aiello,[*,†] Mariateresa Badolato,[†] Federica Pessina,[‡] Claudia Sticozzi,[⊥] Vanessa Maestrini,[§] Carlo Aldinucci,[‡] Livio Luongo,[#] Francesca Guida,[#] Alessia Ligresti,[▽] Anna Artese,[○] Marco Allarà,[▽] Giosué Costa,[○] Maria Frosini,[§] Aniello Schiano Moriello,[▽] Luciano De Petrocellis,[▽] Giuseppe Valacchi,[⊥] Stefano Alcaro,[○] Sabatino Maione,[#] Vincenzo Di Marzo,[▽] Federico Corelli,[∥] and Antonella Brizzi[*,∥]

[†]Dipartimento di Farmacia e Scienza della Salute e della Nutrizione, Università della Calabria, Edificio Polifunzionale, 87036 Arcavacata di Rende, Cosenza, Italy

[‡]Dipartimento Medicina Molecolare e dello Sviluppo, [§]Dipartimento Scienze della Vita, and [∥]Dipartimento Biotecnologie, Chimica e Farmacia, Università di Siena, Polo Scientifico S. Miniato, 53100 Siena, Italy

[⊥]Dipartimento Scienza della Vita e Biotecnologie, Università degli Studi di Ferrara, Via L. Borsari 46, 44121 Ferrara, Italy

[#]Dipartimento di Medicina Sperimentale, Sezione di Farmacologia "L. Donatelli", Seconda Università di Napoli, 80138 Napoli, Italy

[▽]Istituto di Chimica Biomolecolare, Endocannabinoid Research Group, Consiglio Nazionale delle Ricerche, Via Campi Flegrei 34, 80078 Pozzuoli, Napoli, Italy

[○]Dipartimento di Scienze della Salute, Università degli Studi "Magna Graecia" di Catanzaro, Viale Europa, 88100 Catanzaro, Italy

Supporting Information

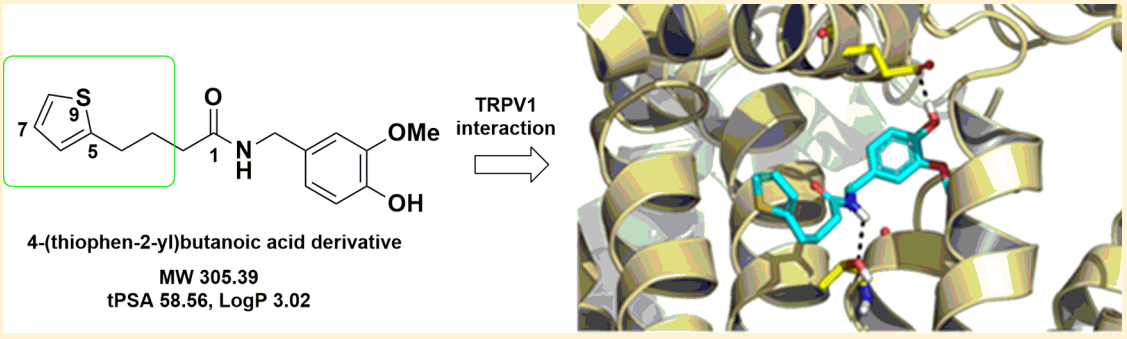

ABSTRACT: 4-(Thiophen-2-yl)butanoic acid was identified as a cyclic substitute of the unsaturated alkyl chain of the natural ligand, capsaicin. Accordingly, a new class of amides was synthesized in good yield and high purity and their molecular recognition against the target was investigated by means of docking experiments followed by molecular dynamics simulations, in order to rationalize their geometrical and thermodynamic profiles. The pharmacological properties of these new compounds were expressed as activation (EC_{50}) and desensitization (IC_{50}) potencies. Several compounds were found to activate TRPV1 channels, and in particular, derivatives **1** and **10** behaved as TRPV1 agonists endowed with good efficacy as compared to capsaicin. The most promising compound **1** was also evaluated for its protective role against oxidative stress on keratinocytes and differentiated human neuroblastoma cell lines expressing the TRPV1 receptor as well as for its cytotoxicity and analgesic activity in vivo.

KEYWORDS: *TRPV1 ligands, capsaicin, antioxidant, oxidative stress, neuroprotective, antinociceptive*

The TRPV1 is a nonselective cation channel with high Ca^{2+} permeability, abundantly expressed in sensory neurons and in higher brain structures, involved in pain processing and neurogenic inflammatory response. In fact, TRPV1 is a

Received: December 16, 2015
Accepted: March 4, 2016
Published: March 4, 2016

DOI: 10.1021/acschemneuro.5b00333
ACS Chem. Neurosci. 2016, 7, 737−748

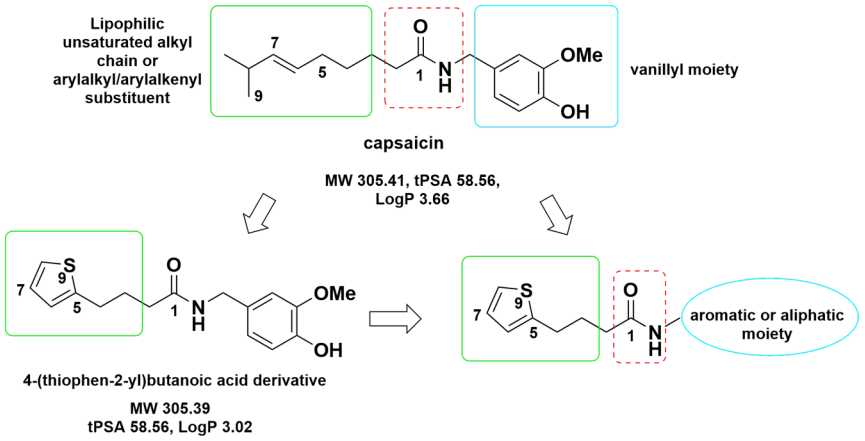

Figure 1. Critical chemical features and general structure of the new synthesized compounds.

Scheme 1. Synthetic Pathways to Obtain the Designed Amides 1−18

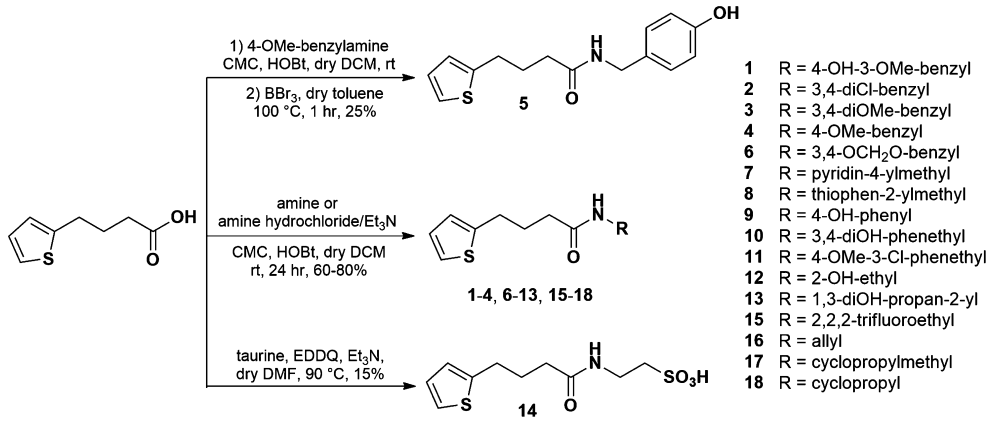

polymodal nociceptor upregulated during chronic pain conditions and exhibits a dynamic threshold of activation that could be significantly lowered by inflammatory conditions such as mild acidification, temperatures over 43 °C and various, mostly noxious, natural products.[1] Among these, the natural pungent principle capsaicin was the first TRPV1 agonist described and its potential analgesic effects were known long before to the identification of its receptor.[2] Capsaicin (*trans*-8-methyl-*N*-vanillyl-6-nonenamide) is a crystalline, lipophilic, colorless, and odorless compound found primarily in the *Capsicum* fruit,[3] responsible for its spicy flavor. Its action is unique in that the initial stimulation of the receptor is followed by a lasting refractory state, traditionally termed desensitization, silencing the whole nerve terminal.[4] However, capsaicin's pungency limits its use in clinical trials, so that the characterization and extraction/synthesis of nonpungent analogues is still in progress. Available experimental evidence indicates that vanilloid agonists, exerting their antinociceptive actions through TRPV1 receptor-mediated selective neurotoxic/neurodegenerative effects directed against somatic and visceral C-fiber nociceptive primary afferent fibers, might be part of analgesic drugs which do not cause addiction and tachyphylaxis.[5] Hence, TRPV1 channels have become a promising pain relief drug target, representing the key mediator in pain processing and neurogenic inflammatory response,[6] and have opened the door for development of new type of analgesics. Nevertheless, capsaicin and related compounds, called capsaicinoids, display a broad spectrum of pharmacological and physiological actions only in part receptor-dependent. Their antioxidant properties, owing to some structural requirements (vanillyl substitution pattern) for free radical-scavenging activity,[7] also contribute to the beneficial effects exhibited by these natural compounds,[8] and a wide range of pathological conditions may benefit from capsaicin-derived agents, such as cancer, inflammation, and cardiovascular diseases.

The structure of capsaicin provided the basis for developing structure−activity relationship for small-molecule TRPV1 modulators, both agonists and antagonists. Three structural features have been identified as critical for receptor interaction as shown in Figure 1. The lipophilic moiety (nonenyl chain for capsaicin), replaceable by an alkyl/alkenyl chain, may be bringing a terminal aromatic nucleus,[9] the polar head (3-methoxy-4-hydroxybenzyl portion), and the linker (an amide for capsaicin, an ester for resiniferatoxin).[10] Both H-bond donor/acceptor aromatic substituents on the vanillyl moiety are important for a potent agonist activity and, in particular, the 4-phenolic hydroxy group represents a crucial pharmacophoric element,[9] while the lipophilicity is relevant for the bioactivity, since TRPV1 agonists need to cross the cell membrane to reach their target.[11]

The aim of this study was to design and synthesize a novel class of TRPV1 ligands endowed with potential agonist or antagonist activity and characterized by a 4-(thiophen-2-yl)butanoic acid amide moiety instead of the nonenoyl chain of capsaicin. In fact, capsaicin is a moderately flexible molecule characterized by a double bond, whose geometry (*trans* in the natural compound, *cis* in the synthetic derivative civamide)[12] does not seem crucial for receptor interaction. Moreover, several studies[13] suggest that

DOI: 10.1021/acschemneuro.5b00333
ACS Chem. Neurosci. 2016, 7, 737−748

Table 1. Results of TRPV1 Assay of Compounds 1−18[a]

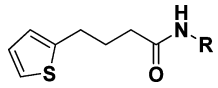

Comp.	R	TRPV1[b] (efficacy)	TRPV1 EC_{50} (μM)	TRPV1[c] IC_{50}(μM)
1	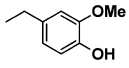	**79.6 ± 1.0**	**0.87 ± 0.06**	**1.60 ± 0.40**
2	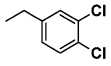	22.8 ± 0.15	1.14 ± 0.05	6.35 ± 0.52
3	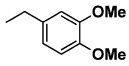	55.1 ± 0.59	5.52 ± 0.23	6.29 ± 0.26
4	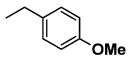	14.7 ± 0.10	n.a.[d]	> 100
5	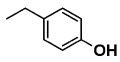	54.0 ± 0.46	4.67 ± 0.19	5.45 ± 0.20
6	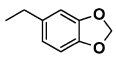	< 10	n.a.	> 100
7		34.4 ± 0.66	14.02 ± 1.22	32.53 ± 0.82
8		11.8 ± 0.10	n.a.	76.86 ± 0.71
9	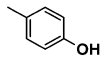	61.0 ± 1.5	37.00 ± 3.7	67.9 ± 0.40
10	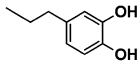	63.0 ± 0.1	15.30 ± 2.9	32.1 ± 1.60
11	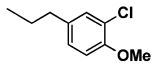	< 10	n.a.	> 20
12	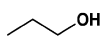	<10	9.10 ± 0.1	> 100
13	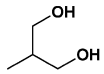	<10	n.a.	> 100
14		26.6 ± 0.1	10.95 ± 0.1	> 100
15		n.a.	n.a.	> 100
16		n.a.	n.a.	> 100
17		7.7 ± 0.1	9.10 ± 0.1	> 100
18		n.a.	n.a.	> 100
Capsaicin		78.6 ± 0.6	0.0053 ± 0.0004	0.0080 ± 0.0003

[a]Data are means ± SEM of $N = 3$ determinations. [b]As percent of the effect of ionomycin (4 μM). [c]Determined against the effect of capsaicin (0.1 μM) after a 5 min preincubation with each compound. [d]n.a. = not active.

the side chain of capsaicin interacts with the receptor in a linear and extended conformation. Therefore, the 4-(thiophen-2-yl)butanoic acid has been considered as suitable cyclic substitute of the unsaturated alkyl chain of the natural compound, because it is chemically characterized by an equivalent number of atoms organized in a short but flexible alkyl chain bearing a heteroaryl

DOI: 10.1021/acschemneuro.5b00333
ACS Chem. Neurosci. 2016, 7, 737−748

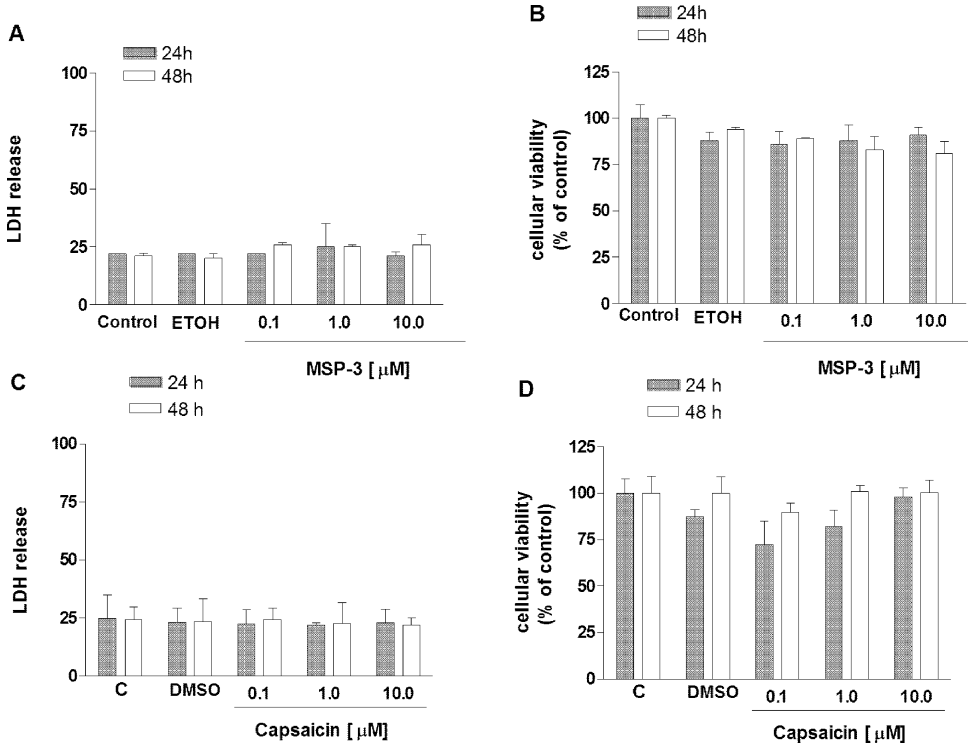

Figure 2. Cytotoxicity of compound **1** (MSP-3; A and B) and capsaicin (C and D) after 24 and 48 h incubation at concentrations ranging from 0.1 to 10 μM in HaCaT cell line. (A and C) LDH release assay and (B and D) Alamar Blu assay. Data are expressed as mean ± SEM (n = 5). No significant difference was observed between groups (one-way ANOVA with Bonferroni post hoc test).

nucleus. Interestingly, both capsaicin and derivative we designed show identical molecular weight, and similar coefficient partition (log P) and topological polar surface area (tPSA) values (Figure 1), thus underlining potentially similar physicochemical and binding properties. Moreover, in the attempt to investigate the influence of the polar head on biological activity and how the electronic/steric properties of this moiety can affect receptor interaction, a family of new derivatives, characterized by high chemical diversity at the polar end, has been synthesized. The present paper describes the functional TRPV1 activities of the designed new ligands and their structure−activity relationship (SAR) analysis. A molecular modeling analysis, carried out by means of docking and molecular dynamics simulations, allowed to investigate the binding modes of the synthesized ligands against TRPV1 target, indicating compound **1** as the most theoretically promising. For such a compound, herein, we report the results of a wider biological evaluation, including cytotoxicity and viability behavior, its protective role against oxidative stress on HaCaT cells (keratinocytes) and on differentiated human neuroblastoma IMR-32 cell line expressing TRVP1 receptors, and finally, its in vivo analgesic activity.

RESULTS AND DISCUSSION

Chemistry. According to the aforementioned structural requirements, a series of selected aromatic and aliphatic amines were condensed with 4-(thiophen-2-yl)butanoic acid, following different synthetic procedures, as depicted in Scheme 1. Besides vanillyl moiety, several aromatic/heteroaromatic, benzyl and phenethyl amines were selected, some of which characterized by a 4-phenolic hydroxy group (i.e., 4-hydroxyaniline, 4-hydroxybenzylamine, and 3-hydroxytyramine) or by polar substituents (i.e., methoxy and/or chloro, 3,4-methylenedioxo groups), while the introduction of aliphatic amines was pursued in order to obtain derivatives with different H-bond donor/acceptor properties as well as a variable degree of lipophilicity.

Commercial 4-(thiophen-2-yl)butanoic acid was coupled in dichloromethane as solvent with the appropriate commercial amines in the presence of 1-cyclohexyl-3-(2-morpholinoethyl)-carbodiimide (CMC) and 1-hydroxybenzotriazole (HOBt) to give the final amides **1**−**4**, **6**−**13**, and **15**−**18** (yields ranging from 60% to 80%). Demethylation reaction in the crude amide **4** was performed with BBr_3 in refluxing dry toluene, furnishing the desired amide **5**. Alternatively, the coupling between the 4-(thiophen-2-yl)butanoic acid and taurine was achieved using a different activating agent, the N-ethoxycarbonyl-2-ethoxy-1,2-dihydroquinoline (EDDQ), in dry DMF, to give the final amide **14** with an acceptable yield of 15%.

In Vitro and in Vivo Pharmacology. Amides **1**−**18**, and natural agonist capsaicin, were evaluated for their pharmacological behavior toward TRPV1 receptors by a functional assay using human embryonic kidney (HEK293) cells stably over-expressing recombinant human TRPV1.[14] The increase concentration of intracellular calcium was used as a measure of the two effects, and activation (EC_{50}) and desensitization (IC_{50}, determined against the effect of capsaicin after a 5 min preincubation with each compound) potency values were summarized in Table 1. (For concentration−effect curves used to generate EC_{50} and IC_{50} values of compound **1**, see Figures S5 and S6 of the Supporting Information.)

To establish the biological profile of the most interesting TRPV1 ligand **1**, cytotoxicity and viability were evaluated in keratinocytes (HaCaT),[15] by cellular LDH release and Alamar Blue assay, respectively, after treatment with the TRPV1 ligand **1** or capsaicin, as reference compound, at concentrations ranging from 0.1 to 10 μM at 24 and 48 h (Figure 2).

DOI: 10.1021/acschemneuro.5b00333
ACS Chem. Neurosci. 2016, 7, 737−748

The protective role of the same compound against oxidative stress was investigated on two cell lines, in HaCaT cells and differentiated human neuroblastoma IMR-32 cells, expressing TRPV1 receptors. HaCaT cells[16] were treated with glucose oxidase (GO) for 1 h to allow the generation of hydrogen peroxide (H_2O_2) as source of oxidative stress (OS). A consequence of OS is the induction of lipid peroxidation that generates several lipid oxidation products (LOPs) among which the unsaturated aldehyde 4-hydroxy-2-nonenale (HNE) is one of the most reactive and potentially toxic. Therefore, evaluating the formation of HNE protein-adducts in keratinocytes pretreated or not pretreated with compound **1** or capsaicin, can give an indirect measurement of the "antioxidant" properties of the compounds (Figure 3).[17]

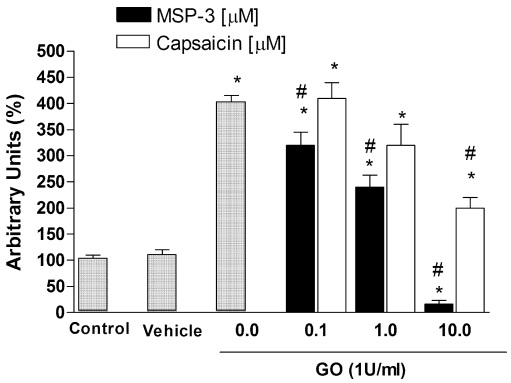

Figure 3. HNE protein-adducts induced by GO treatment in HaCaT cells, measured by Western blot. Data are representative of three experiments. Cells were pretreated with compound **1** (MSP-3) or with capsaicin for 24 h and then treated with GO for 1 h. Quantifications of HNE protein-adduct bands is shown as ratio of HNE/β-actin (bottom panel). Data are expressed as arbitrary units (mean ± SEM, n = 3); statistical analysis was performed by one-way ANOVA followed by Bonferroni post hoc test; $^{*}P < 0.05$ vs control; $^{\#}P < 0.05$ vs GO.

IMR-32 cells were differentiated[18] and then hydrogen peroxide (H_2O_2, 300 μM for 15 h) was used as neurotoxin producing OS resulting in cell death. To assess neuroprotective effects, differentiated neuroblastoma cells expressing TRPV1 receptors[19] were pretreated with test compound **1** or with capsaicin (used as reference compound) at concentrations ranging from 0.1 to 50 μM, and cellular LDH release determined in medium at the end of the experiment (Figure 4). Cell morphology analysis (phase-contrast light microscope) and apoptosis-mediated cell death based on nuclear staining with 4′,6-diamidino-2-phenylindole (DAPI) fluorescent probe (Figure 5) were also performed to further investigate compound **1**-mediated neuroprotection.

Based on the results obtained in the in vitro functional assay, we decided to investigate whether compound **1**, like capsaicin and other TRPV1 agonists, displayed any analgesic activity in vivo.

For this purpose, the formalin test of acute peripheral and inflammatory pain in mice was employed. Formalin-treated mice showed a typical nociceptive behavior characterized by an early, short lasting first phase (0−7 min), followed by a quiescent period, and then a second, prolonged phase (15−60 min) of tonic pain.[20] Test compound (concentrations ranging from 0.0075 to 0.15 μg/paw, 30 μL) was administered 10 min before formalin treatment (1.25%, 30 μL) and lifting, favoring, licking,

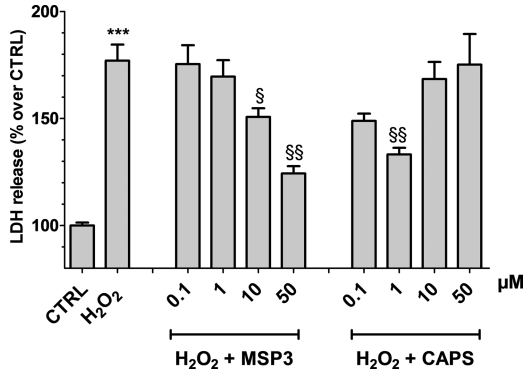

Figure 4. Effects of compound **1** (MSP-3) and capsaicin (CAPS) on H_2O_2-induced LDH release in human neuroblastoma cells. IMR-32 differentiated cells were pretreated with compound **1** or capsaicin for 1 h (0.1−50 μM) prior to 300 μM H_2O_2 for 15 h. Data are reported as mean ± SEM $^{***}P < 0.01$ vs CTRL. $^{\S}P < 0.05$ and $^{\S\S}P < 0.01$ vs H_2O_2 (ANOVA and Bonferroni post hoc test).

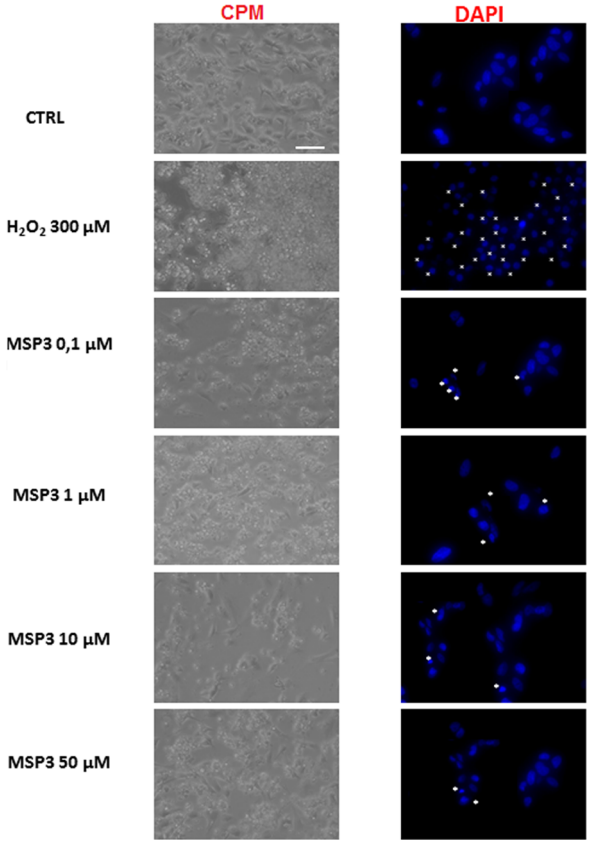

Figure 5. Morphological changes were observed under a contrast-phase microscopy (CPM, scale bar 100 mm, original magnification 100×, left panel); nuclear morphological changes of the cells were observed using a fluorescence microscopy (DAPI staining, right panel, scale bar 100 mm, original magnification 400×).

shaking, and flinching of the injected paw were recorded as nociceptive responses (Figure 6).

Molecular Modeling Analysis. Starting from the 3D homology tetramer model of hTRPV1, kindly provided by Prof. Feng and collaborators,[21] we performed our molecular docking simulations in order to analyze the binding mode and the theoretical affinity of all synthesized compounds. In particular, as reported in Table S3 of the Supporting Information,

DOI: 10.1021/acschemneuro.5b00333
ACS Chem. Neurosci. 2016, 7, 737−748

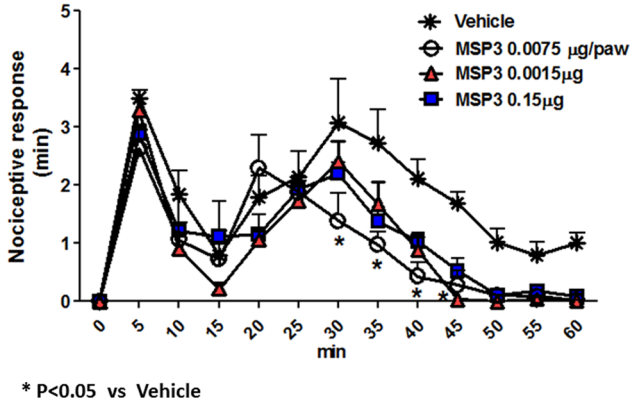

Figure 6. Formalin-treated mice showed a typical nociceptive behavior characterized by an early, short lasting first phase, followed by a quiescent period, and then a second, prolonged phase of tonic pain. Ten minutes before injection of formalin (1.25%, 30 μL), mice received intrapaw administration of either vehicle or compound **1** (MSP-3, 0.0075, 0.015, and 0.15 μg/paw, 30 μL). The total time of the nociceptive response was measured every 5 min and expressed in minutes. The statistical significance was determined by two-way ANOVA followed by a Turkey−Kramer post hoc test. Asterisk (*) indicates significant ($P < 0.05$) differences vs formalin + vehicle-treated animals.

we observed **1**, **2**, **3**, **6**, **9**, and **10** as the most interesting ones, since they were associated with a Glide score (G-Score) similar or better to that of the reference agonist compound capsaicin. More specifically, **1**, **2**, and **10** provided the best theoretical profile and the geometrical analysis of their best poses is reported in Figure 7.

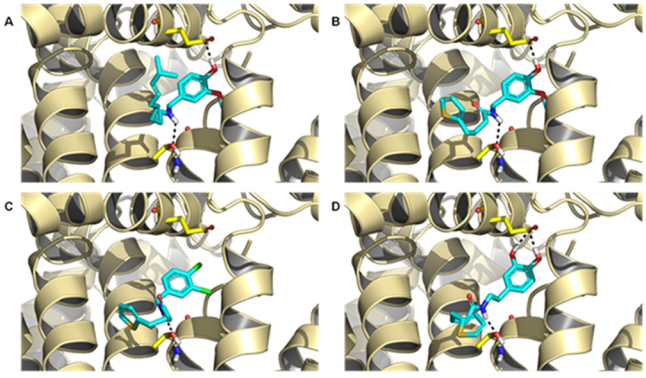

Figure 7. Insight of the (A) capsaicin, (B) **1**, (C) **2**, and (D) **10** TRPV1-template complex showing the hydrogen bonds between the compound and the most involved residues of the protein binding pocket. TRPV1 and its interacting residues are shown, respectively, as light yellow cartoon and yellow carbon sticks; the ligands are represented as cyan carbon sticks. The hydrogen bonds are indicated as black dashed lines.

Compounds **1**, **2**, and **10** reproduced the binding mode of the reference TRPV1 agonist capsaicin, showing a pivotal conserved hydrogen bond (HB) between the amide nitrogen of the ligand and the hydroxyl group of Thr550. Moreover, capsaicin, **1** and **10** were further stabilized by additional HBs between the OH groups of the catechol moiety and Glu570.

Based on the results obtained in the pharmacological experiments, we decided to further investigate compound **1**, since it resulted the most potent TRPV1 agonist. For this purpose, we analyzed the stability of [TRPV1·**1**] complex compared to that of capsaicin by means of 5 ns of molecular dynamics simulations (MDs). By analyzing both compounds, it is clear that capsaicin is conformationally more flexible with respect to **1**; such an evidence was further highlighted by the gyration radius study of both complexes, where the *extendedness* of capsaicin resulted higher if compared to that of **1** (Figure S1 of the Supporting Information). In terms of root means square fluctuation (RMSF), calculated onto the protein side chains, we observed a comparable trend for both complexes (Figure S2 of the Supporting Information), as confirmed by the average obtained values for each TRPV1 residue ($RMSF_{caps}$ = 2.07 Å; $RMSF_1$ = 2.24 Å).

During the MDs, we quantitatively evaluated the single components of the non binding interactions that are crucial for the ligand binding. Specifically, as reported in Figure S3 of the Supporting Information, **1** was well stabilized by several HBs with Tyr511, Thr550 and Glu570 and numerous hydrophobic interactions, especially with Ser512 and Phe591. By contrast, capsaicin binding resulted enhanced by a higher number of hydrophobic contacts to the detriment of HBs. Such an observation was in agreement with our thermodynamic analysis, where capsaicin was associated with a preponderant Van der Waals contribution for its binding affinity, while **1** was well stabilized in TRPV1 pocket especially through electrostatic interactions (Figure S4 of the Supporting Information).

Data obtained from functional assay (see Table 1) revealed that many of the newly synthesized compounds were able to activate TRPV1 channel, confirming our hypothesis that the 4-(thiophen-2-yl)butanoic acid amide moiety is a valuable scaffold for the design of a novel class of TRPV1 ligands. Compounds **1**, **3**, **5**, **9** and **10** are the most interesting compounds showing efficacy values higher than 50% and, in particular, derivative **1**, although less potent (compound **1**, EC_{50} = 870 nM − capsaicin EC_{50} = 5.3 nM) behaved as a good TRPV1 agonist endowed with efficacy similar to that of capsaicin (79.6% and 78.6%, respectively). Concerning the cooperativity behavior, compound **1** showed a Hill coefficient value > 1 (1.095 ± 0.056), but slightly lower compared to that of capsaicin (1.25 ± 0.09); therefore, compound **1** displayed cooperativity, yet to lesser extent than capsaicin. In agreement with structure−activity relationships reported in the literature,[1,9,10] all active compounds possess a phenol moiety though placed at different distance from the amide functionality (see compounds **9**, **5**, and **10**). The natural substitution pattern, the vanillyl moiety, was still optimal for TRPV1 activity, but also 3,4-dichlorobenzyl group was tolerated furnishing a quite potent derivative (compound **2**, EC_{50} = 1.4 μM) although endowed with lower efficacy. On the other hand, the introduction of aliphatic moieties in the amide head caused a considerable loss of binding ability. Cytotoxicity of compound **1** was evaluated in HaCaT cells by measuring LDH release. As shown in Figure 2A, the treatment with compound **1** (at concentrations ranging from 0.1 to 10 μM) did not cause any cytotoxic effect in HaCaT cells both at 24 and at 48 h and similar results were obtained in the presence of capsaicin (Figure 2C). These results were confirmed also by Alamar Blue assay, where no differences in cell viability between control and cells treated with compound **1** (Figure 2B) or with capsaicin (Figure 2D) after 24 and 48 h were observed. The protective role of compound **1** against oxidative stress on both HaCaT cells and differentiated human neuroblastoma (IMR-32) cells was then investigated and compared to that exerted by capsaicin. Normally, human body produces oxygen free radicals (OFR) and other reactive oxygen species (ROS) as by products in

DOI: 10.1021/acschemneuro.5b00333
ACS Chem. Neurosci. 2016, 7, 737−748

numerous physiological processes, primarily as a result of aerobic metabolism. ROS have important beneficial effects under regulated and homeostatic conditions but they are potentially dangerous when produced in excess, because increased oxidative stress can damage biomolecules (proteins, lipids, and DNA), often leading to many chronic diseases, such as cancer, aging, and neurodegenerative disorders. Therefore, compounds endowed with antioxidant activity may have high therapeutic potential and in vitro cell culture studies can be very useful in assessing such properties. In HaCaT cells, as shown in Figure 3, the GO treatment induced a significant increase of HNE protein-adduct levels, effect prevented in a concentration-dependent manner by compound **1** pretreatment. This antioxidant effect was also exhibited by the natural capsaicin, even if with lower efficacy since only the highest concentration (10 μM) was significantly effective. Additionally, in differentiated human neuroblastoma (IMR-32) cells the H_2O_2 treatment induced a significant increase of LDH release, which reached the value of 181.2 ± 9.3% vs controls (Figure 4). The pretreatment with MSP3 (0.1−50 μM), however, restored cell viability in a concentration-dependent fashion. In particular, highest concentrations of compound **1** (i.e., 10 and 50 μM) proved to be maximally effective, as LDH efflux into the medium amounted to 150.7 ± 4.1% ($P < 0.05$ vs H_2O_2) and 124.3 ± 3.4% ($P < 0.01$ vs H_2O_2), respectively. Interestingly, LDH release observed after treatment with 50 μM concentration of compound **1** was not significantly different from that observed in control slices, thus indicating that compound **1** completely reverted H_2O_2 injury. Furthermore, preliminary results obtained by using rat brain cortical slices, an experimental model that maintains the cellular architecture of an intact brain, confirmed the neuroprotective effects of compound **1** (Figure S7 of the Supporting Information).

In differentiated IMR-32 cells the natural TRPV1 agonist capsaicin reverted hydrogen peroxide-induced LDH release. Its effects, however, were not linearly correlated to the concentration used, but followed a U-shaped curve, typical of a hormetic-like effect. The efficacy window was very narrow, since 1 μM capsaicin was the only effective concentration while lower (0.1 μM) or higher (10−50 μM) concentrations were ineffective. Also, in rat cortical slices, subjected to oxidative stress, capsaincin exerted neuroprotection according to a hormetic profile, which was still characterized by a very narrow efficacy window (i.e., 10 μM; see the Supporting Information). The hormetic or biphasic effect of capsaicin was already described in different experimental models,[22,23] and the mechanism underlying this phenomenon could rely on a longer-lasting refractory state of the receptors which might occur at concentration of 10−50 μM capsaicin, leading to a lack in the neuroprotective effects. Alternatively, we can hypothesize that TRPV1 receptor activation at the highest capsacin concentration runs in parallel with the activation of other pathways leading to the suppression of the neuroprotection effect as net, final result. The ability of compound **1** to revert hydrogen peroxide-induced LDH release in a concentration-dependent fashion, along with its stronger antioxidant properties, makes this compound more interesting in terms of neuroprotection and for this reason its effects where further investigated.

Morphological analysis of IMR-32 cells performed at phase-contrast microscopy showed that H_2O_2 caused grade 2 sign of cytotoxicity since about 50% of the cells were round and devoid of intracytoplasmic granules (see Figure 5). Compound **1** significantly attenuated changes caused by H_2O_2 injury as the morphology of IMR-32 cells treated with the highest concentration of the drug was of grade 0−1, that is, low percentage (20%) of round, loosely attached cells and without intracytoplasmic granules. Furthermore, DAPI staining assay showed that DNA fragmentation detected after H_2O_2 exposure was reverted by compound **1** pretreatment (10 and 50 μM).

Lastly, based on the results obtained in in vitro assay, we decided to investigate whether compound **1**, like other TRPV1 agonists and capsaicin, exhibited any analgesic activity in vivo by using the formalin test of peripheral acute and inflammatory pain. Intriguingly, the administration of compound **1** in the range of concentrations used displayed a slight, but significant anti-nociceptive effect by reducing the second phase of the nocifensive behavior induced by formalin treatment (see Figure 6). The effect on the late phase of the formalin, that involves a spinal sensitization, paves the way to investigate this compound in a model of the persistent pain in which several plastic changes occur at spinal and supraspinal levels.

In agreement with the experimental observations, the molecular modeling analysis allowed us to rationalize the better profile of compounds **1**, **2**, **3**, **6**, **9**, and **10**, since also docking simulations showed them as the most promising ones. In particular, as already reported in a recent work,[24] their binding affinity was found to be strictly related to pivotal hydrogen bonds between the vanillyl head and amide neck with residues Glu570 and Thr550 of TRPV1 channel, respectively.

By means of our MDs, we compared the reference TRPV1 agonist capsaicin with the most potent compound **1** both geometrically and thermodynamically, thus detecting similar profiles, according to **1** high efficacy versus TRPV1.

■ CONCLUSIONS

In this study, we have investigated a novel class of chemically stable TRPV1 ligands characterized by the 4-(thiophen-2-yl)butanoic acid amide moiety, starting from the working hypothesis that the long unsaturated side chain of capsaicin could be replaced by a moderately flexible aromatic backbone. Several compounds were found to activate TRPV1 channels, and in particular, derivatives **1** and **10** behaved as TRPV1 agonists endowed with good efficacy as compared to capsaicin. Moreover, compound **1** has turned out to prevent in a concentration-dependent fashion the generation of HNE protein-adducts in HaCaT cells and so to protect keratinocyte cell line by OS damage with more efficacy than the reference compound capsaicin. According to this result, compound **1** dose-dependently prevented also the damage caused by H_2O_2 in differentiated human neuroblastoma cell line as well as rat cortical slices, by completely reverting OS injury at the highest concentration tested and hence showing high neuroprotective effect. On the contrary, capsaicin neuroprotection was limited by a narrow efficacy window, with 1 μM (IMR-32 cells) or 10 μM (rat cortical slices) being the only active concentrations. In vivo results have also highlighted the slight, but significant antinociceptive effect of compound **1** in the second phase of the nocifensive response. Finally, cytotoxicity and cell viability assays confirmed the safe biological profile of compound **1**. Molecular modeling data resulted in agreement with the experimental observations, thus structurally rationalizing the binding mechanism of the most potent **1**.

These results indicate that our novel compounds may represent useful leads for the future development of new TRPV1 ligands and/or of small molecules endowed with protective effects against oxidative stress and with analgesic activity.

DOI: 10.1021/acschemneuro.5b00333
ACS Chem. Neurosci. 2016, 7, 737−748

METHODS

Chemistry. All starting materials, reagents and solvents were purchased from common commercial suppliers and were used as received unless otherwise indicated. Organic solutions were dried over anhydrous sodium sulfate and concentrated with a Büchi rotary evaporator R-110 equipped with KNF N 820 FT 18 vacuum pump. Melting points were determined on a Kofler apparatus (K) or using a Gallenkamp melting point apparatus (G) and are uncorrected. ^{1}H NMR and ^{13}C NMR spectra were recorded in the indicated solvent at 25 °C on a Bruker Advance DPX400 or 300 MHz spectrometer, and chemical shifts were expressed as δ (ppm). The chromatography−mass spectrometry (LC-MS) system consisted of a Triple QuadTM System API 3200 or of an Agilent 1100 series liquid cromatograph system including a 1100 MSD model VL benchtop mass spectrometer with API-ES interface, a binary high-pressure gradient pump (0.4 mL/min low flow rate, employing a binary solvent system of 95/5 methanol/water), and a solvent degassing unit. Nitrogen (purity 99.995%) was used as nebulizer and drying gas. UV detection was monitored at 254 nm. Mass spectra were acquired in positive or negative mode scanning over the mass range m/z of 150−1500. IR spectra were recorded on a PerkinElmer FT-IR Spectrum TWO (Nujol dispersion or $CHCl_3$ solution). The structures of final compounds were unambiguously assessed by ^{1}H NMR, ^{13}C NMR, MS and/or IR. All compounds were checked for purity by TLC on Merck 60 F_{254} silica plates. For column chromatography, Merck 60 silica gel, 230−400 mesh, was used. Final products were purified by a Biotage flash chromatography system with columns 12.25 mm, packed with KP-Sil, 60A, 32−63 μM. Compound purity was assessed by elemental analysis on a PerkinElmer elemental apparatus model 240 for C, H, N, and the data are within ±0.4% of the theoretical values. All the tested compounds possessed a purity of >95.0%.

General Procedure for the Synthesis of Final Amides 1−4, 6−13, and 15−18. To a solution of the appropriate amine (1.5 equiv, or the appropriate amine hydrochloride, 1.5 equiv, and trimethylamine, 2.0 equiv) in dry DCM (10 mL), at room temperature and under nitrogen atmosphere, a solution of the 4-(thien-2-yl)butanoic acid (1.0 equiv) in dry DCM (2.0 mL), solid HOBt (1.2 equiv), and a solution of CMC (1.5 equiv) in dry DCM (3.0 mL) were added, respectively. The mixture was stirred at rt for 24 h. After this time, the solvent was washed twice with a 5% $NaHCO_3$ solution and twice with a saturated NH_4Cl solution. The collected organic layers, dried on anhydrous Na_2SO_4, were concentrated and the crude compound purified by flash chromatograpy on silica gel with the appropriate eluent mixtures.

***N*-(4-Hydroxy-3-methoxybenzyl)-4-(thiophen-2-yl)-butanamide 1.** Eluent: $CHCl_3$/MeOH = 48/2. Yield: 60% as yellow oil. IR (Nujol): 3287, 1645 cm^{-1}. ^{1}H NMR (300 MHz) $CDCl_3$ δ (ppm): 7.04 (dd, 1H, J = 4.0 Hz, J = 1.0 Hz.), 6.9−6.6 (m, 5H), 4.26 (d, 2H, J = 5.6 Hz), 3.78 (s, 3H), 2.80 (t, 2H, J = 7.5 Hz.), 2.19 (t, 2H, J = 7.0 Hz), 2.01−1.91 (m, 2H). ^{13}C NMR (300 MHz) $CDCl_3$ δ (ppm): 172.5, 146.7, 145.1, 144.1, 130.0, 126.7, 124.5, 123.2, 120.7, 114.4, 110.7, 55.9, 43.6, 35.5, 29.0, 27.4. MS (E.I.) m/z: 305 $[M]^+$ (22), 137 (100). Anal. Calcd for $C_{16}H_{19}NO_3S$ (MW 305.39): C, 62.93%; H, 6.27%; N, 4.59%. Found: C, 62.91%; H, 6.28%; N, 4.58%.

Synthesis of *N*-(4-Hydroxybenzyl)-4-(thiophen-2-yl)-butanamide 5. A solution of 4-(thien-2-yl)butanoic acid (1.0 equiv), 4-methoxybenzylamine (1.5 equiv), and *N*-hydroxybenzotriazole (HOBt) (1.2 equiv) in dry DCM (2.5 mL) was cooled at 0 °C and stirred under N_2 atmosphere for 15 min. Thereafter, a solution of 1-cyclohexyl-3-(2-morpholiinoethyl)carbodiimide (CMC) (1.5 equiv) in dry DCM (3.5 mL) was added dropwise. The mixture was stirred at rt for 24 h, then the solvent was washed twice with a 5% $NaHCO_3$ solution, then twice with a saturated NH_4Cl solution, and finally once with brine. The collected organic layers, dried on anhydrous Na_2SO_4, were concentrated and the crude compound used in the next reaction without further purification. To a solution of crude compound (1.0 equiv) in dry toluene, heated at 50 °C for 15 min, was added BBr_3 (4.0 equiv) and the mixture was stirred at 100 °C for 1 h. Afterward, the reaction mixture was allowed to reach room temperature, then cooled to 0 °C and cautiously treated dropwise with H_2O. The organic layer was separated and washed with NaCl saturated solution and 2 N NaOH (3−4 times). The alkaline aqueous phase was treated with concentrated HCl to pH 2 and extracted with Et_2O. The dried and filtered organic layer afforded the pure compound after evaporation of solvent.

Yield: 25% as brown solid. Mp: 105.5 °C (G). ^{1}H NMR (300 MHz) $CDCl_3$ δ (ppm): 6.99 (m, 3H), 6.8−6.5 (m, 4H), 6.10 (br s, 1H), 4.20 (d, 2H, J = 5.4 Hz), 2.75 (t, 2H, J = 7.0 Hz), 2.15 (t, 2H, J = 7,7 Hz), 1.90 (m, 2H). ^{13}C NMR (300 MHz) $CDCl_3$ δ (ppm): 173.2, 156.1, 144.0, 129.2 (×2), 129.1, 126.8, 124.6, 123.2, 115.8 (×2), 43.3, 35.5, 29.1, 27.5. MS (EI) m/z: 275 $[M]^+$ (100). Anal. Calcd for $C_{15}H_{17}NO_2S$ (MW 275.37): C, 65.43%; H, 6.22%; N, 5.09%. Found: C, 65.33%; H, 6.24%; N, 5.10%.

Synthesis of 2-(4-(Thiophen-2-yl)butanamido)-ethanesulfonic acid 14. A solution of 2-aminoethanesulfonic acid hydrochloride (1.1 equiv) and triethylamine (1.4 equiv) in dry DMF (3 mL) was added to a mixture of 4-(thiophen-2-yl)butanoic acid (1.0 equiv) and 2-ethoxy-1-ethoxycarbonyl-1,2-dihydroquinoline (EEDQ) (1.4 equiv) in dry DMF (1.5 mL) and the mixture heated at 90 °C, under N_2, to obtain a clear solution. After cooling to room temperature, the solution was stirred for additional 30 min and then, poured in cold diethyl ether (15 mL) and left to 4 °C overnight. The mixture was decanted and the resinous residue dried under vacuum. The resulting solid was then added to a stirred solution of HCl in methanol (0.85 M, 4.0 equiv) at room temperature. After stirring at rt for 24 h, the suspension was partitioned between chloroform and $NaHCO_3$ saturated solution. The aqueous phase was acidified to pH 6.5 with 1 M HCl and again extracted with chloroform. The organic layers were dried and concentrated to afford a crude material, which was purified by flash chromatography ($CHCl_3$/MeOH 48/2) to give a brown oil (yield 15%).

IR (Nujol): 3500, 1650 cm^{-1}. ^{1}H NMR (300 MHz) $CDCl_3$ δ (ppm): 7.09 (dd, 1H, J = 5.1, J = 1.1 Hz), 6.90 (dd, 1H, J = 5.1, J = 3.4 Hz), 6.79 (m, 1H), 3.70 (m, 2H), 2.98 (m, 2H), 2.85 (m, 2H), 2.22 (t, 2H, J = 5.1 Hz), 1.98 (m, 2H). ^{13}C NMR (300 MHz) $CDCl_3$ δ (ppm): 171.5, 141.1, 126.1, 126.0, 124.0, 41.9, 40.1, 31.9, 29.7, 29.3. MS (E.I.) m/z: 277 $[M]^+$ (13), 256 (27), 129 (39), 73 (100). Anal. Calcd for $C_{10}H_{15}NO_4S_2$ (MW 277.36): C, 43.30%; H, 5.45%; N, 5.05%. Found: C, 43.25%; H, 5.47%; N, 5.03%.

Ligand Preparation. For ligand preparation, the 3D structures of all the studied compounds were generated with the Maestro Build Panel into the graphic interface Maestro Schrödinger ver 10.1.[25] Considering that for an in silico experiment a 3D structure database requires an efficient generation of reasonable, energetically minimized conformations,[26] all ligands were also energy minimized in the absence of the receptor with the OPLS_2005 force field[27] as implemented in the Schrödinger suite, and the lowest energy conformations were used as starting points for the docking simulations.

Target Optimization. An inevitable prerequisite for generating a structure-based model is the knowledge about the ligand-target interaction,[28] including the availability of the 3D structure of the target. Because of the unavailability of a human model of TRPV1, we adopted the 3D coordinates of the model obtained by homology modeling[21] and kindly provided by Prof. Feng.

The preparation procedure of the complex started with "Protein Preparation Wizard"[29] function in Maestro. Hydrogen atoms were added and, finally, the energy minimization calculation was performed using OPLS_2005 force field until the RMSD of all heavy atoms within 0.3 Å.

Docking Simulations. Docking studies of **1−18** toward TRPV1 model were performed by means of Glide software ver. 6.6.[30] The purpose of this method was to develop an exhaustive search in the space of the various positions, orientations, and conformations of each ligand compared to the target.

A semiflexible approach was considered: all flexible 3D ligands were sequentially docked into the binding pocket of the rigid receptors. For the target, using the Receptor Grid Generation panel with the default options, a cubic box of 27 000 Å^3 was defined as binding region, generating the centroid of the most important residues involved in binding of several TRPV1 compounds, as Capsaicin.

For each docking run, we recorded a maximum of 10 poses per ligand; Glide SP protocol was used and the best docked poses for each ligand were selected considering the most negative G-score value.

DOI: 10.1021/acschemneuro.5b00333
ACS Chem. Neurosci. 2016, 7, 737−748

Molecular Dynamics Simulations. Capsaicin and the most interesting TRPV1 agonist **1** were submitted to molecular dynamic simulations (MDs) in order to rationalize the physical basis of the complexes; in fact, MD simulations contain explicit treatment of water and intrinsic receptor flexibility, capturing the dynamic nature of protein−ligand interaction.

The simulation was carried out under the following conditions: recording interval equal to 10 ps; 5 ns of simulation time at 300 K; pressure set to 1 bar; OPLS2005 as force field; and TIP4P[31] water molecules. All simulations were performed by Desmond package[32] and "Simulation Interactions Diagram" panel was used as post-MD analysis tool for exploring protein−ligand interactions.

Desmond "Simulation event analysis" tool was used to monitor, over 5 ns, the root mean square fluctuation (RMSF), calculated onto TRPV1 side chains, the global number of hydrogen bonds (HBs) and hydrophobic interactions established by the ligands with the enzyme, and the interaction energy, in terms of Van der Waals and electrostatic single contributions, of capsaicin and **1**.

The 3D Figures were obtained with PyMOL graphics and modeling package, version 1.7.[33]

Procedure for TRPV1 Channel Assay. HEK293 (human embryonic kidney) cells stably overexpressing recombinant human TRPV1 were grown on 100 mm diameter Petri dishes as monolayers in minimum essential medium (EMEM) supplemented with nonessential amino acids, 10% fetal bovine serum, and 2 mM glutamine, and maintained at 5% CO_2 at 37 °C. Stable expression of channels was checked by quantitative PCR (data not shown). The effect of the substances on intracellular Ca^{2+} concentration ($[Ca^{2+}]_i$) was determined by using Fluo-4, a selective intracellular fluorescent probe for Ca^{2+}. On the day of the experiment, cells were loaded for 1 h at room temperature with the methyl ester Fluo-4-AM (4 μM; Invitrogen) in EMEM without fetal bovine serum, then were washed twice in tyroide's buffer (145 mM NaCl, 2.5 mM KCl, 1.5 mM $CaCl_2$, 1.2 mM $MgCl_2$, 10 mM D-glucose, and 10 mM HEPES, pH 7.4), resuspended in the same buffer, and transferred to the quartz cuvette of the spectrofluorimeter (PerkinElmer LS50B; PerkinElmer Life and Analitycal Sciences, Waltham, MA) under continuous stirring. $[Ca^{2+}]_i$ was determined before and after the addition of test compounds (0.01−100 μM) by measuring cell fluorescence (λ_{EX} = 488 nm, λ_{EM} = 516 nm) at 25 °C. Curve fitting (sigmoidal dose−response variable slope) and parameter estimation were performed with GraphPad Prism (GraphPad Software Inc., San Diego, CA). Potency was expressed as the concentration of test substance exerting half-maximal agonist effect (i.e., half-maximal increases in $[Ca^{2+}]_i$) (EC_{50}). The efficacy of the agonists was first determined by normalizing their effect to the maximum Ca^{2+} influx effect on $[Ca^{2+}]_i$ observed with application of 4 μM ionomycin (Sigma). The values of the effect on $[Ca^{2+}]_i$ in wild type HEK293 (i.e., not transfected with any construct) cells were taken as baseline and subtracted from the values obtained from transfected cells. Antagonist/desensitizing behavior was evaluated against capsaicin (0.1 μM) for TRPV1, by adding the test compounds in the quartz cuvette 5 min before stimulation of cells with agonists. Data are expressed as the concentration exerting a half-maximal inhibition of agonist-induced $[Ca^{2+}]_i$ elevation (IC_{50}), which was calculated again using GraphPad Prism software. The effect on $[Ca^{2+}]_i$ exerted by agonist alone was taken as 100%. Dose response curves were fitted by sigmoidal regression with variable slope. Statistical analysis of the data was performed by analysis of variance at each point using ANOVA followed by the Bonferroni's test.

Keratinocyte Cell Culture and Treatment. HaCaT cells were grown in Dulbecco's modified Eagle's medium High Glucose (Lonza, Milan, Italy), supplemented with 10% FBS, 100 U/mL penicillin, 100 μg/mL streptomycin, and 2 mM L-glutamine as previously described.[16] Cells were incubated at 37 °C for 24 h in 95% air/5% CO_2 until 80% confluency. HaCaT cells were pretreated with compound **1** or capsaicin for 24 and 48 h. The compound was dissolved in DMSO at a concentration of 10 μM as a stock solution. The stock was diluted to the required concentrations directly in the medium. The final concentration of DMSO in culture medium during compounds treatment did not exceed 0.1% (v/v). For HNE protein adducts determination, cells were collected or treated with glucose oxidase (1 U/mL, 1 h) and processed as described below, after treatment with compound **1** or capsaicin.

Keratinocyte Cellular Viability. Viability studies were performed at 24 and 48 h after treatments by Alamar Blue (Resazurin sodium salt from Sigma) and LDH (EuroClone Milan, Italy) release assay. LDH release was measured enzymatically as previously described.[15] Prior to each assay, the cells were lysed with 0.1% (V/V) Triton X-100 in culture media for 30 min at 37 °C to obtain a representative maximal LDH release as the positive control (100% toxicity). Alamar blue stock solution in phosphate buffered saline (pH 7.4, 1 mg/mL) was prepared to obtain final working concentration of 0.1 mg/mL in cell culture medium. Color change of the redox indicator resazurin was measured at 544 nm (excitation) and 590 nm (emission) wavelengths to evaluate oxidized versus reduced forms of the reagent, respectively.

Western Blot Analysis. Total cell lysates were extracted in solubilization buffer containing 50 mM Tris (pH 7.5), 150 mM NaCl, 10% glycerol, 1% Nonidet P-40, 1 mM EGTA, 0.1% SDS, 5 mM *N*-ethylmaleamide (Sigma-Aldrich Corp.), protease, and phosphatase inhibitor cocktails (Sigma-Aldrich Corp.) as previously described.[17] Samples of 60 μg of protein in 3× loading buffer (65 mM Tris base, pH 7.4, 20% glycerol, 2% sodium dodecyl sulfate, 5% β-mercaptoethanol, and 1% bromophenol blue) were boiled for 5 min, loaded onto 10% sodium dodecyl sulfate−polyacrylamide electrophoresis gels and separated by molecular size. The gels were then electroblotted onto nitrocellulose membranes which were then blocked for 1 h in Tris-buffered saline, pH 7.5, containing 0.5% Tween 20 and 5% milk. Membranes were incubated overnight at 4 °C with the primary antibody, goat anti-HNE (Millipore Corporation, Billerica, MA,). Membranes were then incubated with horseradish peroxidase-conjugated secondary antibody (anti-goat) for 1 h, and the bound antibodies were detected using chemiluminescence (BioRad, Milan, Italy). Images of the bands were digitized and the densitometry of the bands were performed using Image-J software.

Differentiated Human Neuroblastoma Cell Line, Reagents, and Culture Conditions. Freely dividing IMR-32 cells (American Type Culture Collection, Rockville, MD) were routinely cultured in 75 cm^2 flasks in 20 mL of medium in 95% air and 5% CO_2 atmosphere at 37 °C and fed (i.e., refreshed medium) at 2 day intervals. The growth medium comprised Eagle Minimum Essential Medium supplemented with 2 mM L-glutamine, 10% heat-inactivated fetal bovine serum (FBS), 100 UI/mL penicillin, and 0.01 mg/mL streptomycin. When confluent, the cells were detached by washing with 0.25% trypsin solution and 0.53 mM EDTA in phosphate-buffered saline preheated to 37 °C. The suspension was centrifuged (1250*g*, 5 min), and the cells were replated at 2.5 × 10^5 cells/mL. After 48 h, cells were differentiated according to Rao and Kisaalita[18] by the addition of 10 μM of 5-bromo-deoxyuridine (BrdU). The differentiation medium was completely refreshed every 2 days for 2 weeks.

Drug Treatment and Differentiated Human Neuroblastoma Cell Viability Assessment. To assess neuroprotective effects, IMR-32 differentiated cells were treated for 1 h with compound **1** or capsaicin (0.1−50 μM), and thereafter H_2O_2 (300 μM) was added to the medium for 15 h. Control cell cultures were treated with vehicle (DMSO 0.01%). Cell viability was determined by measuring LDH activity in cell supernatant (Cytotoxicity Detection Kit, Roche), and data expressed as the percentage of LDH released, assuming that of control cells 100%. Moreover, in order to register defects in integrity and cellular density undetected by the LDH assay, IMR-32 differentiated cells were examined by using a phase-contrast light microscope. The results were evaluated using the grade scale, described in USP 28 (United States Pharmacopeia edition 2005) (grades 0−4) for assessment of the cytotoxic potential of tested materials, as follows: grade 0, no reactivity (discrete intracytoplasmic granules, no cell lysis); grade 1, slight reactivity (no more than 20% of the cells are round, loosely attached and without intracytoplasmic granules; occasional lysed cells are present); grade 2, mild reactivity (no more than 50% of the cells are round and devoid of intracytoplasmic granules, no extensive cell lysis and empty areas between cells); grade 3, moderate (up to 70% of cells are rounded or lysed); grade 4, severe (nearly complete destruction of the cells). Finally, assessment of apoptosis based on nuclear morphology was

DOI: 10.1021/acschemneuro.5b00333
ACS Chem. Neurosci. 2016, 7, 737−748

performed using the 4′,6-diamidino-2-phenylindole (DAPI) staining kit (Life Tecnologies Italia, Monza, Italy) according to the manufacturer's protocol, with slight modifications.[20] At the end of drug treatment, cells were rinsed with ice-cold PBS buffer and immediately fixed with 4% paraformaldehyde (30 min, 25 °C) followed by three washings with PBS. PBS/Triton (0.2% v v^{-1}) was then added (10 min, 25 °C) and afterward cells were stained with DAPI. After washing again with distilled water, cells were placed on a slide for fluorescence microscopy with the antifade mounting medium 1,4-diazabicyclo octane in glycerol (DABCO) and examined by a reverse-phase microscope (Leica Microsystems, Wetzlar, Germany). Nuclei with fragmented and condensed DNA were scored as apoptotic cells.

Rat Brain Slices and Hydrogen Peroxide-Induced Injury. All animal care and experimental protocols conformed to the European Union Guidelines for the Care and the Use of Laboratory Animals (European Union Directive 2010/63/EU) and were approved by the Italian Department of Health (813/2015-PR). The experimental protocols used were already described.[34,35] Briefly, male Wistar rats (250−300 g; Charles River Italia, Calco, Italy) were killed by decapitation, and the brain quickly removed and placed in artificial cerebrospinal fluid (ACSF) with the following composition (in mM): 120 NaCl; 2 KCl; 1 $CaCl_2$; 1 $MgSO_4$; 25 HEPES; 1 KH_2PO_4; and 10 glucose, adjusted to pH 7.4 and previously bubbled with a 95% O_2−5% CO_2 gas mixture for 20−30 min. The cortex was dissected and cut into 400 μm thickness slices by using a manual chopper (Stoelting Co., Wood Dale, IL). Slices were then transferred into 24-well culture plates containing 0.5 mL of ACSF/well and left at room temperature (25 °C) for 60 min in order to recover from slicing trauma. During this period, the medium was removed and replaced with fresh, oxygenated ACSF every 15 min. Afterward, slices were treated with ACSF containing (or not, in case of controls) compound **1** or capsaicin (0.1−50 μM) for 60 min at 30 °C. After this period, the medium with drugs was mantained and hydrogen peroxide (10 μM for 60 min) was added to the medium at 30 °C in a water bath.

Brain Slice Viability Assays: MTT and Tissue Edema. Slice viability assay was performed by the colorimetric [3-(4,5-dimethylthiazol-2-yl)-2,5-diphenyl tetrazolium bromide] (MTT) method. In particular, slices were washed with ACSF, incubated with 0.5 mg/mL of MTT (300 μL in the same 24 multiwell) at 37 °C for 45 min. Then slices were gently transferred to a 96 multiwell, with 200 μL of DMSO added, and incubated for 30 min at 37 °C in a shaking plate. After incubation, 100 μL of supernatant was prelevated, and the formazan product measured at 560 and 630 nm (OD560−OD630). Cell viability was expressed as a percentage of untreated cells or slices (controls). Statistical significance was assessed by using ANOVA (ordinary or repeated measures followed by Dunnett or Bonferroni post test) (GraphPad Prism version 5.04, GraphPad Software Inc., San Diego, CA). In all comparisons, the level of statistical significance (P) was set at 0.05.

Evaluation of Antinociceptive Activity in Mice. Male C57BL/6J mice, 8 weeks old (Harlan, Italy), were housed 5 per cage under controlled illumination (12:12 h light/dark cycle; light on 06.00 h) and standard environmental conditions (room temperature 22 ± 1 °C, humidity 60 ± 10%) for at least 1 week before experimental use. Mouse chow and tap water were available ad libitum. The experimental procedures were in accordance with Italian and European regulations governing the care and treatment of laboratory animals (Permission no. 41/2007B). Animal care was in compliance with Ethical Guidelines of the IASP and European Community (E.C. L358/1 18/12/86) on the use and protection of animals in experimental research. All efforts were made to minimize animal suffering and to reduce the number of animals used. Formalin injection induces a biphasic stereotypical nocifensive behavior.[36] Nociceptive responses are divided into an early, short-lasting first phase (0−7 min) caused by a primary afferent discharge produced by the stimulus, followed by a quiescent period and then a second, prolonged phase (15−60 min) of tonic pain. Mice received formalin (1.25% in saline, 30 μL) in the dorsal surface of one side of the hindpaw. Each mouse was randomly assigned to one of the experimental groups, placed in a Plexiglas cage and allowed to move freely for 30 min. A mirror was placed at a 45° angle under the cage to allow full view of the hindpaws. Lifting, favoring, licking, shaking, and flinching of the injected paw were recorded as nociceptive responses. The duration of these noxious behaviors was monitored by an observer blind to the experimental treatment for periods of 0−10 min (early phase) and 20−60 min (late phase) after formalin administration. Groups of 6−8 animals per treatment were used with each animal being used for one treatment only. Mice received vehicle (5% DMSO in 0.9% NaCl) or different doses of compound **1** (0.0075, 0.015, and 0.15 μg/paw, 30 μL) administered 10 min before the formalin or saline.

■ ASSOCIATED CONTENT

Supporting Information

The Supporting Information is available free of charge on the ACS Publications website at DOI: 10.1021/acschemneuro.5b00333.

Physical and spectral data and elemental analyses for compounds **2**−**4**, **6**−**13**, and **15**−**18**; Table S3 and Figures S1−S4 of molecular dynamics simulations analyses for capsaicin and compound **1**; concentration−effect curves used to generate EC_{50} and IC_{50} of compound 1 (Figures S5 and S6); concentration−effect curves of compound **1**; effects of compound **1** and capsaicin (CAPS) on H_2O_2-induced decrease in rat cortical slice viability (PDF)

■ AUTHOR INFORMATION

Corresponding Authors

*(F.A.) Phone: +39 984 493154. Fax: +39 984 493107. E-mail: francesca.aiello@unical.it.

*(A.B) Phone: +39 577 234329. Fax: +39 577 234333. E-mail: antonella.brizzi@unisi.it.

Author Contributions

A.B., F.A., F.C., and M.B. developed the chemical synthesis, performed the fully instrumental characterization and their interpretation of all new molecules described in the manuscript. Thus, they wrote the relative chemical and experimental parts of the manuscript and S.I. and drafted the Main Body of the manuscript. C.S. performed experiments and data analysis on HaCat cells. F.P. performed data analysis, interpretation, study supervision, and drafted part of the article on citotoxicity and oxidative stress. G.V. studied, supervised, and drafted part of the article on citotoxicity and oxidative stress. V.M. and C.A. performed experiments and data analysis on IMR-32 cells. M.F. studied, supervised, and performed interpretation of data on citotoxicity experiments. L.L., S.M., and F.G. performed in vivo assays. A.L., V.D.M., L.d.P.M.A., and A.S.M. developed, executed, and performed interpretation of TRPV1 test and enzymatic assays. A.A., G.C., and S.A. carried out the molecular modeling, and docking experiments.

Funding

Authors from the University of Siena wish to thank Sienabiotech S.p.A. (Sienabiotech Grant 2012) for financial support. S.M. would like to thank the Ministero dell'Istruzione, dell'Università e della Ricerca (MIUR, PRIN 2012, Prot. No. 2012WBSSY4_001) for financial support and Regione Campania that funded this research under POR Campania FESR 2007-2013-O.O. 2.1. (FarmaBioNet). G.C. was supported by the "Research grant entitled to the memory of Anna and Ninì Barbieri".

Notes

The authors declare no competing financial interest.

DOI: 10.1021/acschemneuro.5b00333
ACS Chem. Neurosci. 2016, 7, 737−748

■ ACKNOWLEDGMENTS

Thanks are also due to Professor Zhiwei Feng for providing the starting 3D homology tetramer model of hTRPV1.

■ ABBREVIATIONS

TRPV1, transient receptor potential vanilloid type-1; ClogP, calculated coefficient partition; tPSA, topological polar surface area; SAR, structure−activity relationship; HaCaT, human keratinocyte cell line; IMR-32, human neuroblastoma cell line; CMC, 1-cyclohexyl-3-(2-morpholinoethyl)carbodiimide; HOBt, 1-hydroxybenzotriazole; EDDQ, *N*-ethoxycarbonyl-2-ethoxy-1,2-dihydroquinoline; DMF, dimethylformamide; HEK293, human embryonic kidney cell line; LDH, lactate dehydrogenase; GO, glucose oxidase; OS, oxidative stress; LOPs, lipid oxidation products; HNE, 4-hydroxy-2-nonenale; DAPI, 4′,6-diamidino-2-phenylindole; HB, hydrogen bond; MDs, molecular dynamics simulations; RMSF, root means square fluctuation; OFR, oxygen free radicals; ROS, reactive oxygen species

■ REFERENCES

(1) Di Marzo, V., and De Petrocellis, L. (2010) Endocannabinoids as Regulators of Transient Receptor Potential (TRP) Channels: a Further Opportunity to Develop New Endocannabinoid-Based Therapeutic Drugs. *Curr. Med. Chem. 17*, 1430−1449.

(2) Rebolledo, C. L., Sotelo-Hitschfeld, P., Brauchi, S., and Olavarría, M. Z. (2013) Design and synthesis of conformationally restricted capsaicin analogues based in 1,3,4-thiadiazole heterocycle reveal a novel family of transient receptor potential vanilloid 1 (TRPV1) antagonists. *Eur. J. Med. Chem. 66*, 193−203.

(3) Reyes-Escogido, M. L., Gonzalez-Mondragon, E. G., and Vazquez-Tzompantzi, E. (2011) Chemical and Pharmacological Aspects of Capsaicin. *Molecules 16*, 1253−1270.

(4) Szallasi, A., and Blumberg, P. M. (1999) Vanilloid (Capsaicin) Receptors and Mechanisms. *Pharmacol. Rev. 51*, 159−211.

(5) Jancsó, G., Oszlács, O., and Sántha, P. (2011) The Capsaicin Paradox: Pain Relief by an Algesic Agent. *Anti-Inflammatory Anti-Allergy Agents Med. Chem. 10*, 52−65.

(6) Jansson, E. T., Trkulja, C. L., Ahemaiti, A., Millingen, M., Jeffries, G. DM., Jardemark, K., and Orwar, O. (2013) Effect of cholesterol depletion on the pore dilation of TRPV1. *Mol. Pain 9*, 1−9.

(7) Rice-Evans, C. A., Miller, N. J., and Paganga, G. (1997) Antioxidant properties of phenolic compounds. *Trends Plant Sci. 2*, 152−159.

(8) Luo, X.-J., Peng, J., and Li, Y.-J. (2011) Recent advances in the study on capsaicinoids and capsinoids. *Eur. J. Pharmacol. 650*, 1−7.

(9) Wrigglesworth, R., Walpole, C. S., Bevan, S., Campell, E. A., Dray, A., Hughes, G. A., James, I., Masdin, K. J., and Winter, J. (1996) Analogues of Capsaicin with Agonist Activity as Novel Analgesic Agents: Structure-Activity Studies. 4. Potent, Orally Active Analgesics. *J. Med. Chem. 39*, 4942−4951.

(10) Lee, J. H., Lee, Y., Ryu, H., Kang, D. W., Lee, J., Lazar, J., Pearce, L. V., Pavlyukovets, V. A., Blumberg, P. M., and Choi, S. (2011) Structural insights into transient receptor potential vanilloid type 1 (TRPV1) from homology modelling, flexible docking, and mutational studies. *J. Comput.-Aided Mol. Des. 25*, 317−327.

(11) Ursu, D., Knopp, K., Beattie, R. E., Liu, B., and Sher, E. (2010) Pungency of TRPV1 agonists is directly correlated with kinetics of receptor activation and lipophilicity. *Eur. J. Pharmacol. 641*, 114−122.

(12) Wong, G. Y., and Gavva, N. R. (2009) Therapeutic potential of vanilloid receptor TRPV1 agonists and antagonists as analgesics: recent advances and setbacks. *Brain Res. Rev. 60*, 267−277.

(13) (a) Jordt, S.-E., and Julius, D. (2002) Molecular basis for Species-Specific Sensitivity to "Hot" Chili Peppers. *Cell 108*, 421−430. (b) Winkler, M., Moraux, T., Khairy, H. A., Scott, R. H., Slawin, A. M. Z., and O'Hagan, D. (2009) Synthesis and Vanilloid Receptor (TRPV1) Activity of the Enantiomers of α-Fluorinated Capsaicin. *ChemBioChem 10*, 823−828.

(14) Brizzi, A., Aiello, F., Marini, P., Cascio, M. G., Corelli, F., Brizzi, V., De Petrocellis, L., Ligresti, A., Luongo, L., Lamponi, S., Maione, S., Pertwee, R. G., and Di Marzo, V. (2014) Structure-affinity relationships and pharmacological characterization of new alkyl-resorcinol cannabinoid receptor ligands: Identification of a dual cannabinoid receptor/TRPA1 channel agonist. *Bioorg. Med. Chem. 22*, 4770−4783.

(15) Sticozzi, C., Belmonte, G., Cervellati, F., Di Capua, A., Maioli, E., Cappelli, A., Giordani, A., Biava, M., Anzini, M., and Valacchi, G. (2013) Antiproliferative effect of two novel COX-2 inhibitors on human keratinocytes. *Eur. J. Pharm. Sci. 49*, 133−141.

(16) Valacchi, G., Rimbach, G., Saliou, C., Weber, S. U., and Packer, L. (2001) Effect of benzoyl peroxide on antioxidant status, NF-kappaB activity and interleukin-1alpha gene expression in human keratinocytes. *Toxicology 165*, 225−234.

(17) Valacchi, G., Davis, P. A., Khan, E. M., Lanir, R., Maioli, E., Pecorelli, A., Cross, C. E., and Goldkorn, T. (2011) Cigarette smoke exposure causes changes in Scavenger Receptor B1 level and distribution in lung cells. *Int. J. Biochem. Cell Biol. 43*, 1065−1070.

(18) Rao, R. R., and Kisaalita, W. S. (2002) Biochemical and electrophysiological differentiation profile of a human neuroblastoma (IMR-32) cell line. *In vitro Cell Dev. Biol. Anim. 38*, 450−456.

(19) Abdullah, H., Heaney, L. G., Cosby, S. L., and McGarvey, L. P. (2014) Rhinovirus upregulates transient receptor potential channels in a human neuronal cell line: implications for respiratory virus-induced cough reflex sensitivity. *Thorax 69*, 46−54.

(20) Brizi, C., Santulli, C., Micucci, M., Budriesi, R., Chiarini, A., Aldinucci, C., and Frosini, M. (2016) Neuroprotective Effects of Castanea sativa Mill. Bark Extract in Human Neuroblastoma Cells Subjected to Oxidative Stress. *J. Cell. Biochem. 117*, 510−520.

(21) Feng, Z., Pearce, L. V., Xu, X., Yang, X., Yang, P., Blumberg, P. M., and Xie, X. Q. (2015) Structural insight into tetrameric hTRPV1 from homology modeling, molecular docking, molecular dynamics simulation, virtual screening, and bioassay validations. *J. Chem. Inf. Model. 55*, 572−588.

(22) Lee, J. G., Yon, J. M., Lin, C., Jung, A. Y., Jung, K. Y., and Nam, S. Y. (2012) Combined treatment with capsaicin and resveratrol enhances neuroprotection against glutamate-induced toxicity in mouse cerebral cortical neurons. *Food Chem. Toxicol. 50*, 3877−3885.

(23) Marini, E., Magi, G., Mingoia, M., Pugnaloni, A., and Facinelli, B. (2015) Antimicrobial and Anti-Virulence Activity of Capsaicin Against Erythromycin-Resistant, Cell-Invasive Group A Streptococci. *Front. Microbiol. 6*, 1281.

(24) Yang, F., Xiao, X., Cheng, W., Yang, W., Yu, P., Song, Z., Yarov-Yarovoy, V., and Zheng, J. (2015) Structural mechanism underlying capsaicin binding and activation of the TRPV1 ion channel. *Nat. Chem. Biol. 11*, 518−524.

(25) Schrodinger LLC. (2015) *Maestro*, version 10.1, Schrödinger, LLC, New York.

(26) Kirchmair, J., Laggner, C., Wolber, G., and Langer, T. (2005) Comparative analysis of protein-bound ligand conformations with respect to catalyst's conformational space subsampling algorithms. *J. Chem. Inf. Model. 45*, 422−430.

(27) Jorgensen, W. L., Maxwell, D. S., and Tirado-Rives, J. (1996) Development and testing of the OPLS all-atom force field on conformational energetics and properties of organic liquids. *J. Am. Chem. Soc. 118*, 11225−11236.

(28) Congreve, M., Murray, C. W., and Blundell, T. L. (2005) Structural biology and drug discovery. *Drug Discovery Today 10*, 895−907.

(29) (a) Schrodinger LLC. (2015) *Schrödinger Suite 2015−1 Protein Preparation Wizard*, Epik version 3.1 Schrödinger, LLC, New York. (b) Schrodinger LLC. (2015) *Impact*, version 6.6, Schrödinger, LLC, New York. (c) Schrodinger LLC. (2015) *Prime*, version 3.9 Schrödinger, LLC, New York.

(30) Schrodinger LLC. (2015) *Glide*, version 6.6 Schrödinger, LLC, New York.

(31) (a) Jorgensen, W. L., Chandrasekhar, J., Madura, J. D., Impey, R. W., and Klein, M. L. (1983) Comparison of simple potential functions for simulating liquid water. *J. Chem. Phys. 79*, 926−935. (b) Jorgensen,

DOI: 10.1021/acschemneuro.5b00333
ACS Chem. Neurosci. 2016, 7, 737−748

W. L., and Madura, J. D. (1985) Temperature and size dependence for monte carlo simulations of TIP4P water. *Mol. Phys. 56*, 1381−1392.
(32) (a) *Desmond Molecular Dynamics System*, version 4.1 (2015) D. E. Shaw Research, New York. (b) Schrodinger LLC. (2015) *Maestro-Desmond Interoperability Tools*, version 4.1, Schrödinger, New York.
(33) Schrodinger LLC. (2015) *The PyMOL Molecular Graphics System*, Version 1.7.0.0. Schrödinger, LLC, New York.
(34) Quincozes-Santos, A., Bobermin, L. D., Tramontina, A. C., Wartchow, K. M., Tagliari, B., Souza, D. O., Wyse, A. T., and Gonçalves, C. A. (2014) Oxidative stress mediated by NMDA, AMPA/KA channels in acute hippocampal slices: neuroprotective effect of resveratrol. *Toxicol. In Vitro 28*, 544−551.
(35) Contartese, A., Valoti, M., Corelli, F., Pasquini, S., Mugnaini, C., Pessina, F., Aldinucci, C., Sgaragli, G., and Frosini, M. (2012) A novel CB2 agonist, COR167, potently protects rat brain cortical slices against OGD and reperfusion injury. *Pharmacol. Res. 66*, 555−563.
(36) Abbott, F. V., and Guy, E. R. (1995) Effects of morphine, pentobarbital and amphetamine on formalin-induced behaviours in infant rats: sedation versus specific suppression of pain. *Pain 62*, 303−312.

DOI: 10.1021/acschemneuro.5b00333
ACS Chem. Neurosci. 2016, 7, 737−748